Efficient Fault Detection Technique for Brushless DC Motor using Electrical Signature Analysis (ESA)

Submitted by:

Farhan Ahmed Butt: 2011-MS-EE-79

Supervised by: Dr. Syed Abdul Rahman Kashif

Department of Electrical Engineering

University of Engineering and Technology, Lahore

November, 2015

Efficient Fault Detection Technique for Brushless DC Motor using Electrical Signature Analysis (ESA)

Submitted to the Faculty of Electrical Engineering of the University of Engineering and Technology Lahore
in partial fulfilment of the requirements for the Degree of

Master of Science
In
Electrical Engineering

Thesis approved on November, 2015.

Dr. Syed Abdul Rahman Kashif (Supervisor)	(External Examiner)
Chairman Department of Electrical Engineering	Dean Faculty of Electrical Engineering

Department of Electrical Engineering
University of Engineering and Technology, Lahore

Declaration

I, Farhan Ahmed Butt, declare that the work presented in this thesis is my own.

Signed:_____

Date:_____

Acknowledgments

All praise is for Allah, the most Beneficent and the most Merciful. He has provided us the means to learn and grow in our limited understanding of the universe.

I would like to thank my supervisor Dr. Syed Abdul Rahman Kashif, whose patient attention and knowledgeable guidance has always been present at every stage of this work. Without his help and wisdom, this work would not have been possible.

I would like to thank Dr. Muhammad Asghar Saqib for his guidance and thoughtful advice on various problems that I encountered during this project.

I would thank my Family, especially my parents whose prayers have been always with me.

I would thank my friends, for their well wishes and support.

I dedicate this work to my parents, whose prayers have always been with me.

Table of Content

List of Figures

List of Tables

List of Abbreviations

BLDC	Brushless Direct Current
ESA	Electrical Signature Analysis
DSP	Digital Signal Processing
DC	Direct Current
DAQ	Data Acquisition
ADC	Analogue to Digital Converter
MOSFET	Metal Oxide Field Effect Transistor
RPM	Revolutions per Minute

Abstract

BLDC motors are widely used in industrial processes due to their compact size, reduced electro-magnetic interference and constant torque characteristics. Condition monitoring and incipient fault detection of BLDC motors are becoming very important to reduce the machine interruption for unscheduled repair and maintenance, reflecting in reduced cost and enhanced quality of the mechanical procedures. Correct identification, exact area, and timely recognition of incipient faults help maintain a strategic distance from harmful, some of the time devastative results on the system under study. Electrical signature analysis (ESA) provides the capability of detecting problems in the connections, misalignments and rotor-stator eccentricities. It is just like the warning light in the car dashboard and works as preventative-maintenance tool. The proposed technique is capable of detecting stator faults under dynamic mechanical stresses on the system. The Performance is evaluated empirically by comparing harmonics under different load conditions. The "Steady state dynamic model" has been implemented to validate the empirically obtained results. The comparison and condition monitoring is executed by observing the spectrum of stator currents under varying load conditions.

Chapter - 1

Introduction

Electrical machines are extensively used in the industrial processes. Presently, permanent magnet brushless DC (BLDC) motors are the business' need because of their exceptionally effective operation, lower support expense and little size when contrasted with the conventional motors. Their real time condition monitoring and incipient fault detection is of the main concern for their continuous operation [1], [2].

Electrical signature analysis (ESA) is isolated and non-intrusive technique to detect fault in the hardware under test. Information procurement takes not as much as a minute per motor hence it is time productive. Real time current and voltage information are obtained specifically from the motor, while the hardware is in operation. The gathered information can be used to determine the phase imbalance, motor load, power factor, power harmonics, and the effect of the driven hardware on the motor. ESA likewise assesses rotor and stator health and rotor-stator eccentricity (air gap) characteristics. In addition, degradation of the bearings from the traces can also be observed. ESA is particularly helpful in accessing mechanical conditions it is unrealistic or advantageous to make measurements when the hardware is vibrating.

Shortcoming recognition in electric engines and drive frameworks is a point that has procured discriminating consideration. Right finding, exact area, and early location of incipient faults help evade destructive and infrequent devastative results on the framework under thought. On-line condition checking and diagnostics could naturally set up repair arranges and time span. Likewise, machine downtime for unscheduled support could be minimized, which can decrease the expense as well as improve the unwavering quality of the mechanical procedure [3].

Recent trends in the area of machine-fault diagnosis have employed various digital signal-processing (DSP) devices to extract fault signatures from characteristic waveforms that could recognize the deficiency. Feature extraction performed in the frequency domain possesses high

resistance to time-domain deceiving phenomena such as noise and switching transients. Online real-time condition observing is vital for every mechanical procedure to proactively secure the hardware and lessen procedure down time and the related expenses. For BLDC engines, online observing is particularly basic to avert serious harm to the delicate procedures and to decrease the repair cost. Early detection of BLDC defects at beginning stages can greatly reduce the risk of disastrous failure and also lessen the effective downtime needed for the fixation [4].

1.1 Literature review

The literature review is presented in this section.

1.1.1 Importance of electrical machines

Electrical machines are basically electro-mechanical energy conversion devices converting the electrical energy to mechanical energy and vice versa. More than 70% of the energy is generated by the conversion of mechanical energy to electrical energy and finally 70% of all the electrical energy generated is converted back to mechanical energy. it shows the importance of electrical machines in the field of electrical engineering. There are different types of electrical machines that are in use. Although, their operating principal is somewhat similar but they are very different in terms of construction and usage [1].

1.1.2 DC motor

A DC electrical motor converts DC electrical energy into mechanical energy. DC machine consist of a magnetic frame or yoke which protects it from the external disturbances. It houses field system and maintains the armature through bearings. Stator magnets are electromagnets having adjacent poles with opposite polarity. They perform the function of producing the magnetic field. Armature is an arrangement of conductors and coils that are allowed to pivot on the supported bearings. The armature comprise of different parts. The armature core is comprised of high permeability dainty silicon substance steel animations. External fringe of armature core comprise of openings to carry

armature windings which are for the most part comprised of copper wire and are twisted over the armature core.

The commutator is cylindrical and comprised of copper. It performs two basic functions, firstly it collects current from the armature conductors and secondly converts the alternating current of the armature into uni-directional current. This is done by using the brushes are made up of carbon or graphite. Their main function is collecting the current from the moving commutators. Shaft is the turning piece of the DC motor. We acquire the last yield as mechanical energy from the shaft. The armature is mounted on the shaft. At the point when the outside source is connected to the brushes, the current begins flowing into the armature which builds up a force in the armature because of the impact of the magnetic field in the stator whose direction is given by Fleming left hand principle. Due to the development of this force in every armature conductor, the armature will turn in the clock wise direction and subsequently the shaft also begins rotating. Finally, the output power is acquired from the shaft [5].

1.1.3 Brushless DC motor (BLDC)

BLDC motors are very popular in automobile industry, medical devices and aerospace engineering as they have no mechanical commutators and slip rings because switching is performed electronically. As a result there is reduced electromagnetic interference and sparking due to absence of mechanical brushes. Three-phase DC motor drive system is used to control the phase sequence and duty cycle of the operation of BLDC motor.

A brushless DC motor consist of almost same components with inside out construction including a control circuitry, on the back side of the base. The brushless DC motors have this major drawback that they need a controller circuit to operate. There is usually one controller chip and a set of FET transistors which control the power flow in the coils.

In order to make the operation more reliable, productive and less boisterous the recent trend has been to make use of brushless DC motors. They are light in comparison to brushed motors of same output power. The brushes in conventional DC motors are always in contact which may cause

sparking and ionizing spikes, thus for operation that require long life cycles and reliability the brushed DC motors should never be used. The rotor of BLDC motor has permanent magnets and the stator has the windings. By applying DC power to the coil, the coil becomes an electro-magnet. The basis of operation of the BLDC motor is simple force interaction between the permanent and the electro-magnet. The opposite poles of the rotor and the stator are attracted to each other when the coil energizes in this condition. As the rotor reaches near this coil, the next coil pair is energized and the rotor permanent magnet is attracted toward this electro-magnet. After completion of this cycle, the coils are energized with the opposite polarity. This process is repeated and the rotor continue to rotate [1], [2], [3], [5].

The major drawback of the BLDC motor is that the two dead coils reduce the power output remarkably as only one coil pair is energized at any instant. The problem can be resolved via adopting a methodology that when the coil in front of the permanent magnet attracts the rotor electromagnet behind the rotor is energized in a manner that it repels it. This combined effect generates more torque and output power from the motor. It also make sure that the BLDC has a constant torque nature. With this configuration the two coils needs to be energized separately but by making a small modification to the stator coil, the process is simplified. In this case we just connect the free ends of the coils together. Then these work as they are separately energized. In this case to get the information about which coil pair is to be energized at any time is to get the continuous rotation of BLDC motor. An electronic controller is used for this purpose. The position of the rotor is located by a sensor, and on this basis the controller decides which coil pair is to be energized. Usually for this purpose, Hall Effect sensors are used. BLDC motor could be an in-runner style or out-runner style. In-runner BLDC motor contains rotor which rotates inside of stator while in out-runner BLDC motor the rotor rotates outside of stator.

Two algorithms can be implemented for the control of BLDC motor i.e. a sensor based or a sensorless algorithm. In sensor based algorithm Hall Effect sensors are used to find the position of the rotor windings, for the synchronism of the electrical excitation with the rotor position. After getting the position of the next rotor pair to be energized, motor is commuted to the next switch pair. While in sensorless algorithm, we determine the commutation time by sensing back-EMF

voltages. Commutation depends totally on the position of the rotating magnet. Two phases of the BLDC motor are always active while the third phase remains in floating condition.
The complete working and operating principal of BLDC motor with all the control schemes and algorithms is already described in literature [5].

1.1.4 Brushless DC motor (BLDC) control

For the operation of the BLDC motor, there must be some rotating magnetic field. Normally a three-phase permanent magnet BLDC motor consisting of three stator windings that are energized as two at a time to create a rotating magnetic field is used for the purpose. This method is somewhat easy to implement but to prevent the rotor from getting locked with the stator, the energization of the stator must be sequenced while keeping in mind the exact positions of the north and South Pole of rotor magnets. The information about the position could be received from shaft encoders or from Hall Effect sensors that detect the position of the rotor magnet. For a typical, three-phase, sensor based BLDC motor operation, there are six different sectors of commutation in which two specific phases are energized [1], [5].

1.1.5 Electrical signature analysis (ESA)

Electric signature analysis (ESA) is a technique used for condition, monitoring and incipient fault detection in motors, generators and transformers. By using ESA we can identify electrical and mechanical faults in electrical equipment when they are in operation. As a preventive-maintenance tool, Electrical Signature Analysis can be used for analyzing the performance of many different equipment's in operation.

We can also identify several mechanical and electrical problems; rotor-stator eccentricity, bearing failures, stator winding short circuits and misalignments. It is a more preventive and predictive approach towards the incipient fault detection and gives us a level of redundancy.

As already mentioned, the electric signature analysis (ESA) and condition monitoring techniques both are used for studying faults in electrical equipment's so in electrical motor's the ESA provides

the ability to identify connection problems and rotor-stator eccentricity (air gap) characteristics. If the rotor-stator eccentricity misaligns then it will cause the vibrations in motor. As these vibrations will possess a certain pattern which will repeat itself due to the periodic nature of motor operation. These vibrations will affect the electrical signature of BLDC motor and cause the periodic noise in the signal. As mentioned earlier, frequency domain possesses strong immunity to time-domain signal processing. These vibrations which seem to be a noise in time domain possess a certain frequency domain signature. By just eliminating the healthy signature out of this faulty signature we can get the required results [3], [4], [6], [7].

ESA is a portable, remote and non-invasive technique. Its whole assembly is invisible to the monitored equipment. Data acquisition is very simple and it takes less than three minutes to get all the required signatures of voltage or currents out of the BLDC motor. The biggest advantage of this technique is that it works while the equipment is in operation. So we don't need to stop the operation to perform electrical signature analysis. The compiled data can help us determine the problems in rotor demagnetization, phase imbalance, motor load, power factor, power harmonics and the impact of the driven equipment on the motor. ESA also assesses rotor as well as stator health and rotor-stator eccentricity (air gap) characteristics. In addition, the bearings condition can also be observed by the data obtained. ESA is particularly helpful in accessing mechanical conditions when it is not possible or convenient to make vibration measurements.

The voltage and current based fault detection in BLDC motors is already discussed in literature [4].

1.1.6 Condition monitoring

On-load condition monitoring and incipient fault detection is the topic that has recently acquired a lot of attention. As mentioned already that the equipment is invisible to the measuring unit we don't have to shut down the machine operation to get the status of their health; on-load condition monitoring can use either vibration analysis or electrical signature analysis technique. By real time analysis we could identify the faults before they escalates into something critical. Hence, machine down time could be minimized reflecting in less cost of the complete operation cycle [8].

Recent trends in the area of health diagnosis of electrical machines utilized new digital signal processing techniques to extract the faulty signature of the machine. In case of time domain the added noise in the signatures could mislead to wrong results. While in frequency domain, every signal possess a particular pattern. So we could easily identify and separate the faulty signature out of healthy signature and we could benchmark these signatures for the future comparison [8], [9].

Condition based monitoring services improves the availability and reliability of the equipment under consideration. Dynamic forces have a direct impact on the internal working of the electrical machines. These have to withstand many strains over thousands of operating hours during their life time. Any breakdown would substantially diminish the profitability of the machine unit. To prevent the occurrence of any damage their condition monitoring is very important. The system monitors the condition of the rotating parts inside the electrical machine. It requires sensors to be attached to the equipment under test. Sensors measure vibrations caused by the enormous forces. The information gathered by the sensors is digitalized and recorded. After that the data get analyzed. Bearings and other components oscillates at a certain frequency. The frequency could be calculated based on the geometry of the bearing. If any fault occurs in the machine it would indicate a specific signature in the analysis. Condition monitoring allows us to reduce the down time of the electrical machines by half and gear repairs can be quickly planned. Cutting down time by half increases efficiency bare by boosting the economic viability of the electrical machine. Condition monitoring can be applied to more than just mechanical components so that no damage is overlooked during the maintenance to reduce the down time [10], [11].

By condition monitoring we minimize the risk through early fault detection. As we are aware of the fact that rotating machine and the static electrical equipment give rise to different indications that the problem is developing then if diagnose those problems in enough time and can react to them [12]. There are lot of in which we can analyze e.g.

1. Vibration analysis
2. Ultrasound analysis
3. Thermography analysis

4. Partial discharge analysis
5. Electrical signature analysis

The inspection and observation both are an important part of condition monitoring. The basic principal behind condition monitoring is that we run the test for a certain period of time when the equipment is running in its normal healthy state so that we could say it is running defect free. Then at a certain point we can say that there is the ability to detect that the condition is degrading and the fault has developed. In some cases ultrasound is the first technique that is employed to detect any defect in the rotating electrical equipment. As it has the ability to locate any lubrication problems. But generally speaking, during initial stages bearing does not make any sound. The earlier we pick it up the lower risks associated with the failure of the equipment and lower the cost of dealing with the problem. [13], [14], [15].

The basic application of the condition monitoring is the fault detection, maintenance, planning, and avoidance of secondary damage or collateral damage and reduced spares inventory. After consideration of these point there are fewer safety incidents both in terms of the equipment failing and environmental point of view. In that case we can plan the maintenance in a better way and that would reflect the improved safety higher likelihood of having less down time and greater availability of spare equipment. We either let the equipment fail via getting the advanced warning of the failure, or fix it before it fails. It avoids catastrophic failures and reduces the likelihood that a machine will fail catastrophically. The aim of reliability improvement is to run a plant with the lowest cost, at the highest availability. After detection of the root cause of the fault and conditions that will result in failure and reduced reliability, proactive measures can be taken. The failure can be a cause of unbalance, poor installation, misalignment, soft foot, lubrication, turbulence and cavitation. Poor lubrication increase friction in the rotating parts, operating it incorrectly puts all kinds of load on the bearings, shields and shafts. They all result in bearing failure, reduced efficiency, and seal failure, coupling failure, shaft failure, leaks and contamination. From a condition monitoring point of view we need to detect the occurrence of these conditions. If we detect those issues and correct them then we are less likely to get bearing faults.

Chapter - 2

The Theoretical and Empirical Analysis of Harmonics in Brushless DC motor

The first part of this chapter gives detail on experimental setup that is used to evaluate the harmonic contents present in current drawn stator current of brushless DC (BLDC) motor. Latter part of this chapter is dedicated to explaining the BLDC motor equivalent model.

2.1 Fault Classification

We cannot design a system which would never fail, but we can minimize the risk of failure by its performance monitoring analysis. In order to access the health we need to know how many different types of faults which could arise in BLDC motor. The faults can be divided into three main categories.

- Rotor Faults
    1. Dynamic eccentricity problems
    2. Bearing damage
    3. Rotor permanent magnet fault
    4. Asymmetries in the rotor
- Stator Faults
    1. Short circuit of stator winding

2. Open circuiting of stator winding
3. Heating effect (change of stator resistance)

- Inverter Faults
    1. Inverter switch short circuit
    2. Inverter switch open circuit

2.2 Brushless DC motor structure

Among all fault categories, rotor faults are most likely to occur. As all the mechanical parts are in contact with each other so misalignment usually happens. The BLDC motor used in the experimental setup is shown in the Figure 1.1. It is a 12-pole three-phase permanent magnet brushless DC motor. Stator winding, rotor magnet and bearing are clearly visible in the Figure 1.1.

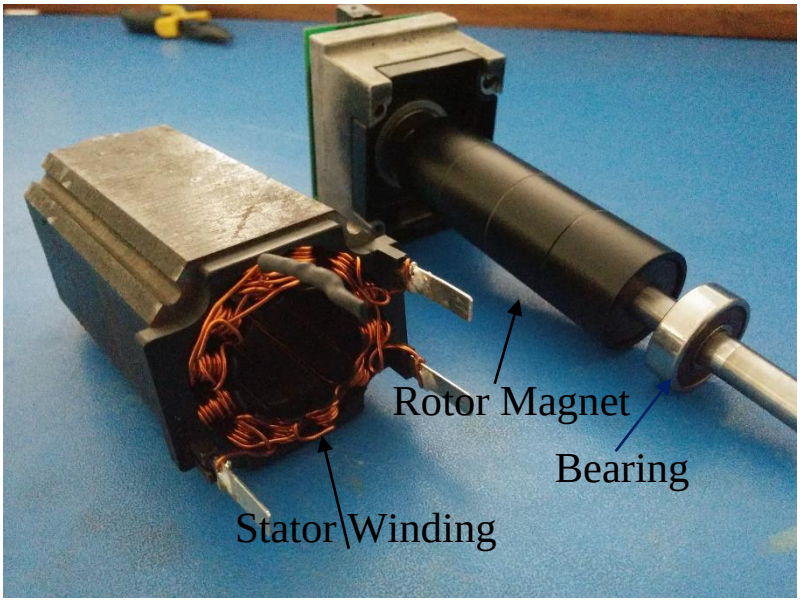

Figure 1.1: A 12-pole three-phase permanent magnet brushless DC motor.

As discussed in the chapter that the BLDC motor requires a circuitry to control its operation. The control circuitry contains Hall Effect sensors, encoders and three-phase power supply terminals. The control circuitry is shown in the Figure 1.2.

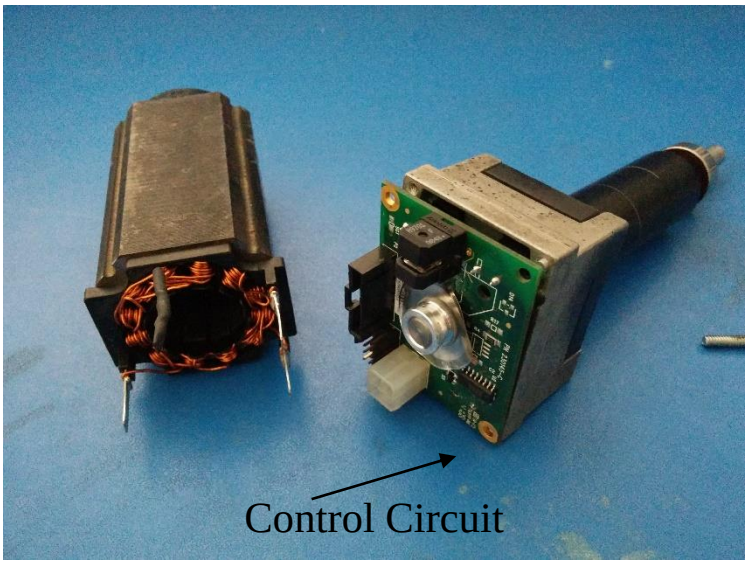

Figure 1.2: Control circuitry for 12-pole three-phase permanent magnet brushless DC motor.

2.3 BLDC motor generator coupling

A stainless steel platform is used to couple the BLDC motor with the DC series generator as shown in Figure 1.3. DC series generator is used for applying load on the BLDC motor. Electrical load is then connected to series generator. This electrical load is then varied in order to simulate dynamic mechanical stresses on BLDC motor. Balancing screws are also used to adjust the alignment of the platform.

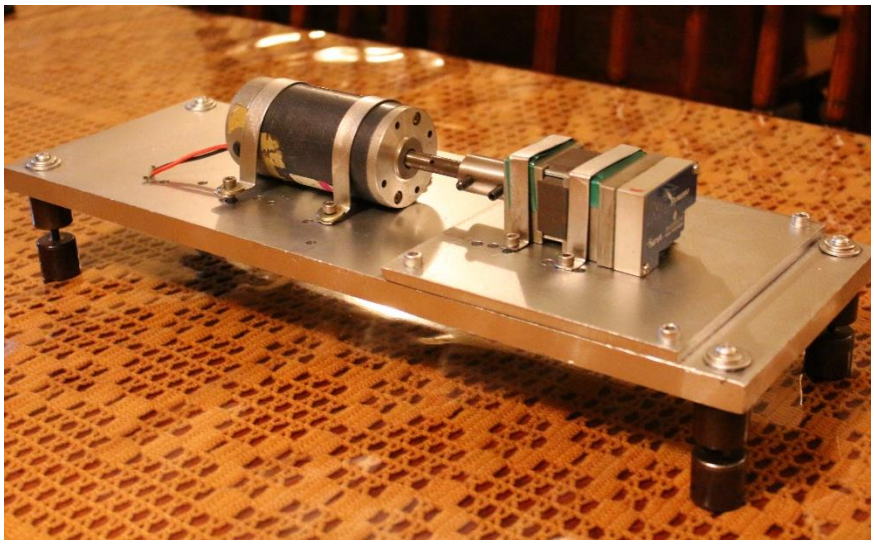

Figure 1.3: A stainless steel platform used to couple the BLDC motor with the DC series generator.

2.4 Winding resistance measurement

To obtain the empirical results the windings resistance of the BLDC motor is measured through precision micro ohm-meter devices available in High Voltage Laboratory. The winding resistance is used to measure if the three-phases of the BLDC motor are balanced. The testing setup for the measurement of the winding resistance is shown in Figure 1.4.

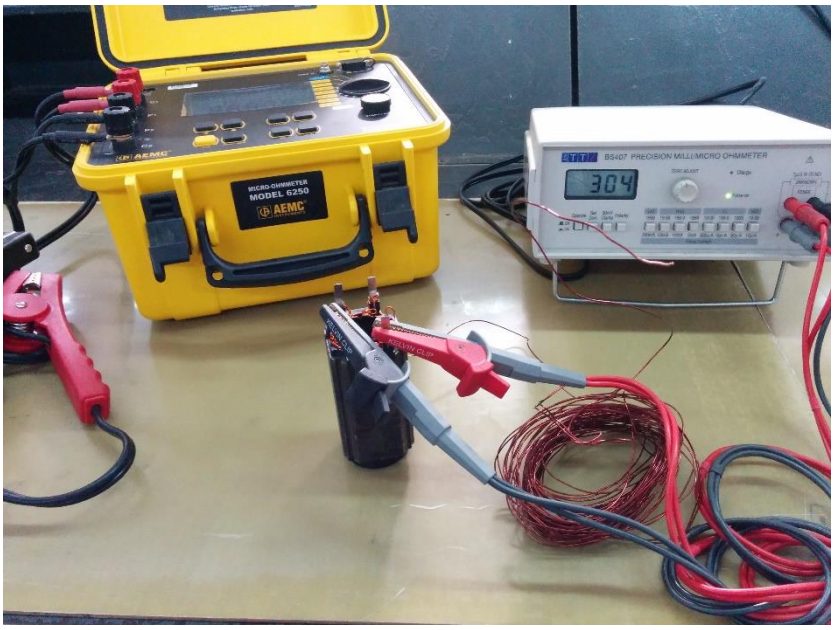

Figure 1.4: The testing setup for finding the winding resistance.

A resistive electrical load as shown in Figure 1.5 is used to apply the electrical load on the generator which in turns apply mechanical load to BLDC motor. Resistive load is connected to DC series generator via ammeter and voltmeter to measure power consumed by the load. So that we can find the input mechanical power of the generator. Input mechanical power of the generator is actually the output mechanical power of the BLDC motor.

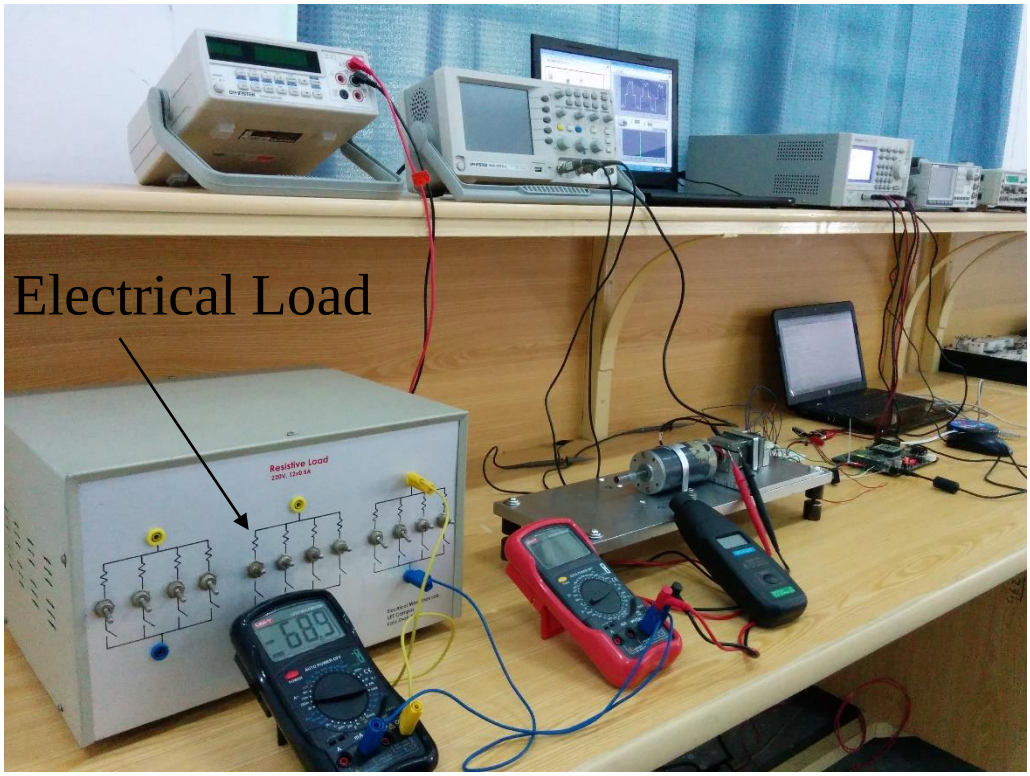

Figure 1.5: The testing setup showing a resistive electrical load.

2.5 Multifunction data acquisition board USB-6009

For the experimental purposes 14-bit, 48kS/s multifunction data acquisition (DAQ) card is used to get the electrical signatures of stator currents as shown in Figure 1.6. The signal obtained by the DAQ is then digitalized.

Figure 1.6: A 14-bit, 48kS/s multifunction data acquisition (DAQ) card.

2.6 BLDC Motor used in the setup

The brushless DC motor used in the experimental setup is of 24 Volt, 26 Watt and 12-pole three-phase ratings. The pin connections are shown in Figure 1.7.

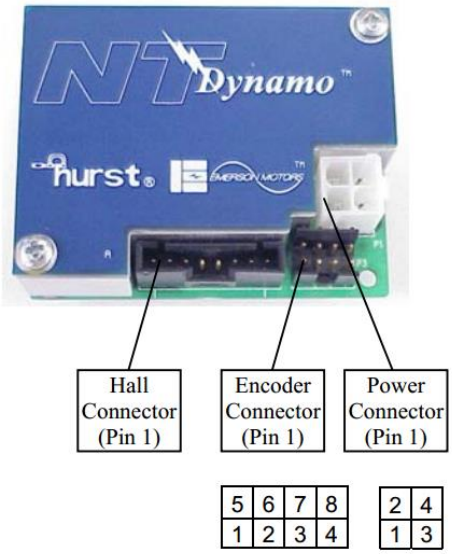

Figure 1.7: The brushless DC motor terminals.

Table 2.1: Connection sheet for BLDC motor

Connector	Pin #	Function
Power	1	Phase C
	2	Phase B
	3	Phase A
	4	Gnd
Hall	1	Vs
	2	Vs (RTN)
	3	Hall S2
	4	Hall S1
	5	Hall S3
Encoder	1	+5Vs
	2	Encoder A
	3	Encoder B
	4	Encoder I
	5	+5Vs (RTN)
	6	Encoder / A
	7	Encoder / B
	8	Encoder / I

2.7 Complete experimental setup

The complete experimental setup for efficient detection of faults in BLDC motor is shown in Figure 1.8. Hall Effect sensor is used for the measurement of the stator line currents of BLDC motor. The signal obtained from the Hall sensor is then digitalized and real time data acquisition is performed.

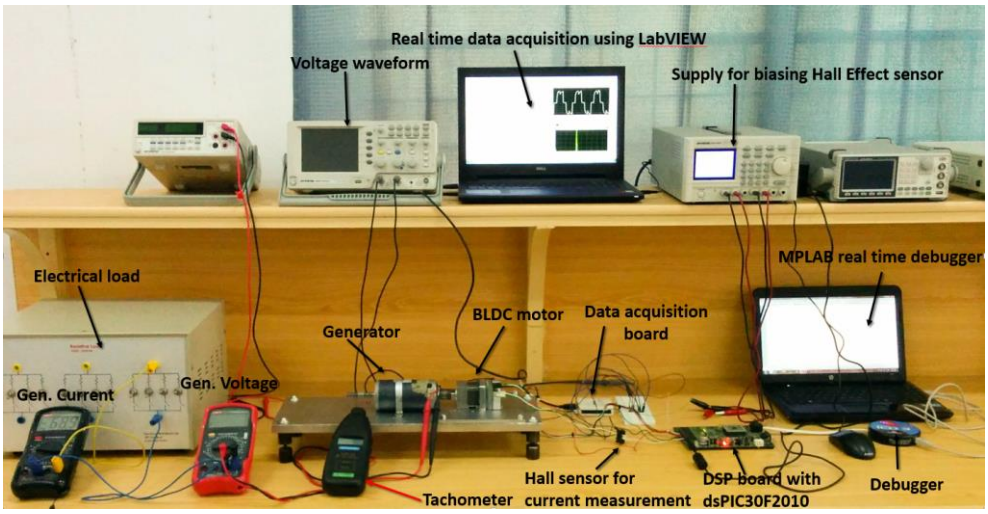

Figure 1.8: The experimental setup for efficient detection of faults in BLDC motor.

2.8 Sensored close loop algorithm

Sensor based closed loop control is implemented using dsPIC digital signal controller as shown in Figure 1.9. The BLDC motor could be adjusted to any desired speed by changing the resistance of the potentiometer available on the dsPIC board. A correlation between rotor speed and time for one electrical cycle is given by equation 2.1.

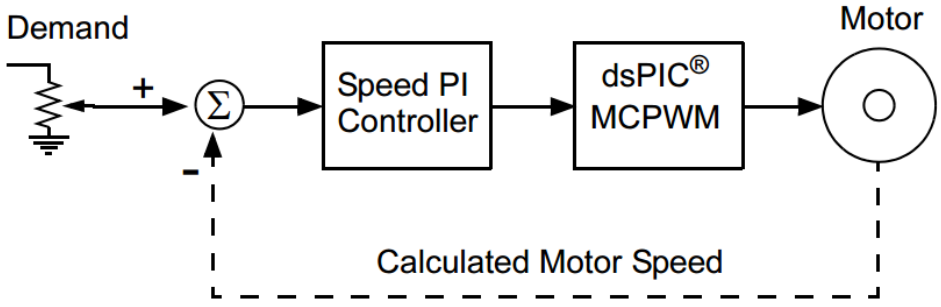

Figure 1.9: A sensor based close loop control implemented using dsPIC digital signal controller.

$$S = \frac{60}{\frac{P}{2} * T} \; rpm \qquad (2.1)$$

Where S is the rotor speed in rpm, P is the number of poles and T is the time for one electrical cycle.

Inserting the value of time for one electrical cycle, the rotor speed is given by equation 2.2.

$$S = \frac{60}{\frac{12}{2} * 0.0041667}\ rpm = 2400 \text{ rpm} \qquad (2.2)$$

Sensor based close loop control algorithm is implemented in the network for driving the BLDC motor. The Figure 1.9 shows the complete flow chart diagram for the sensor based close loop control algorithm that is used in the hardware setup to control the BLDC motor.

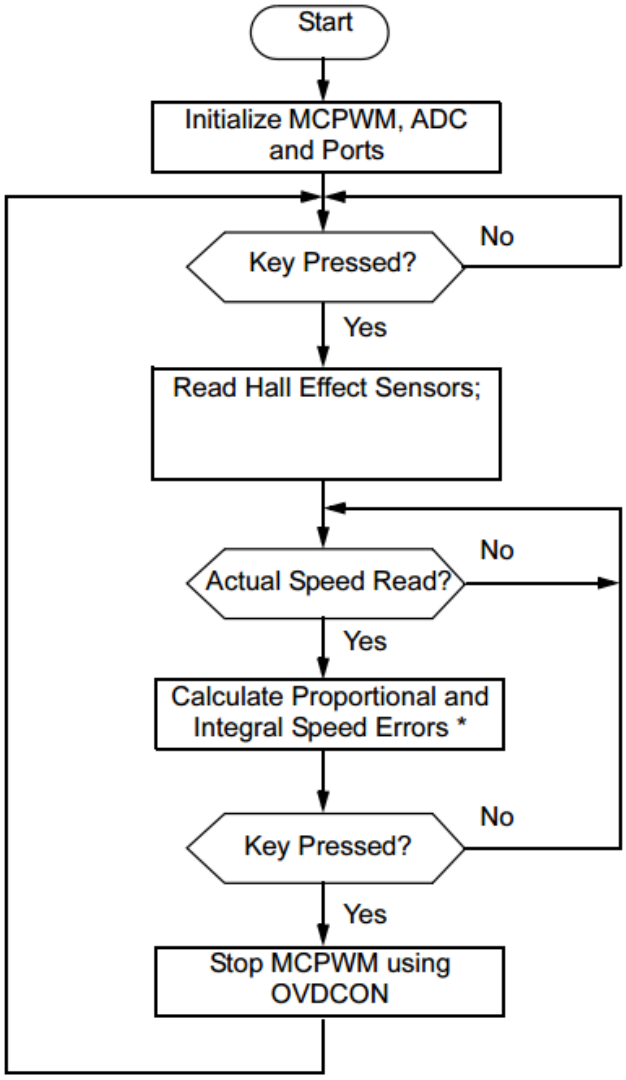

Figure 1.9: Flow chart diagram for the sensor based close loop control algorithm.

2.9 Schematic diagram of drive system

Schematic diagram of the BLDC motor drive used in the setup is shown in Figure 1.10. It comprises of a power supply, filter circuit, control switches and motor. To control the switching logic, MOSFET's are deployed using six-step trapezoidal or 120° commutation is used.

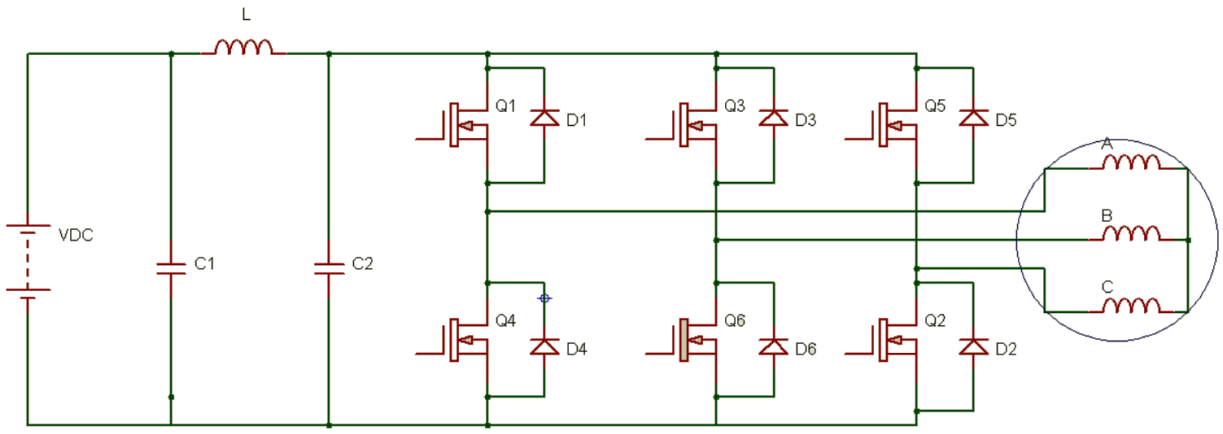

Figure 1.10: Schematic diagram of the BLDC motor drive.

2.10 Control scheme

The 120° commutation or 6-step commutation scheme is used as a control logic for the phase windings shown in Figure 1.11. Each commutation step or sector is equal to 60 electrical degrees. Summing all of the sectors results in one or 360°electrical revolution.

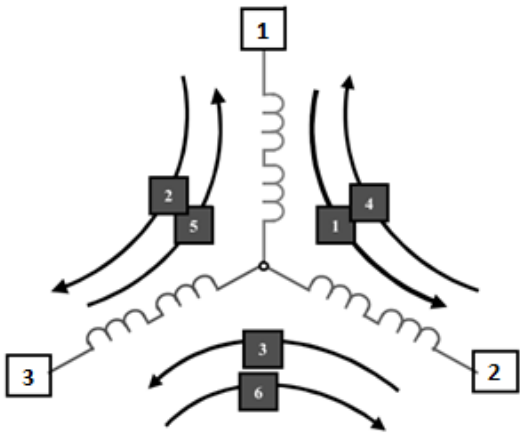

Figure 1.11: A 120° commutation or 6-step commutation scheme used as a control logic.

- Sector one
  - Winding 1 is positive
  - Winding 2 is negative
  - Winding 3 is not used
- Sector two
  - Winding 1 is positive
  - Winding 2 is not used
  - Winding 3 is negative
- Sector three
  - Winding 1 is not used
  - Winding 2 is negative
  - Winding 3 is positive
- Sector four
  - Winding 1 is negative
  - Winding 2 is positive
  - Winding 3 is not used
- Sector five
  - Winding 1 is negative
  - Winding 2 is not driven
  - Winding 3 is positive
- Sector six
  - Winding 1 is not used
  - Winding 2 is negative
  - Winding 3 is positive

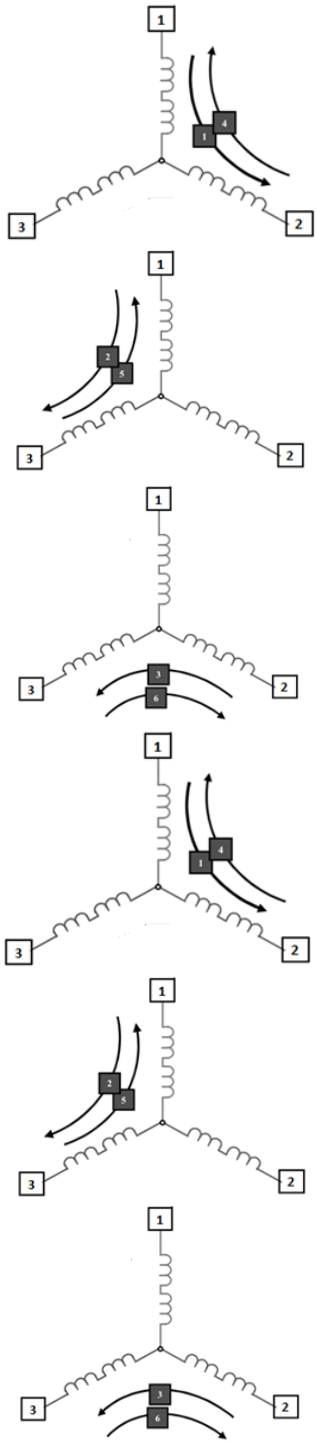

For every single step, two of the windings are excited and one winding is always open/ not used as shown in figure 1.12. We can describe the motor speed in mechanical revolutions per minute and electrical revolution per minutes.

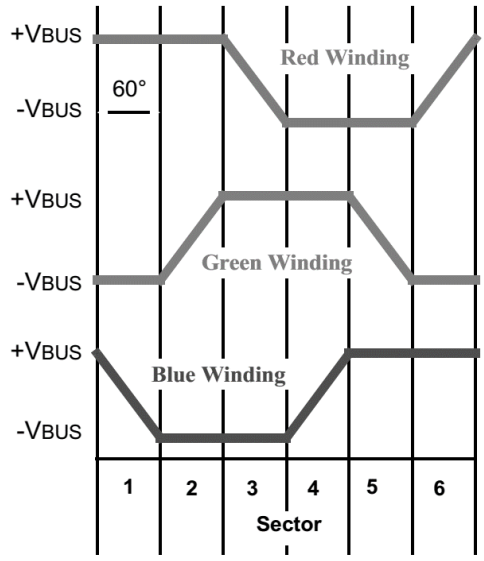

Figure 1.12: A six step commutation scheme.

Similarly, electrical revolutions per minute could be calculated by equation 2.3

$$RPM_{Electrical} = \frac{RPM_{Mechanical} * BLDC\ motor\ poles}{2} \tag{2.3}$$

2.11 Lumped Network Model

In order to evaluate the performance of the drive system a lumped network is implemented as shown in Figure 1.13.

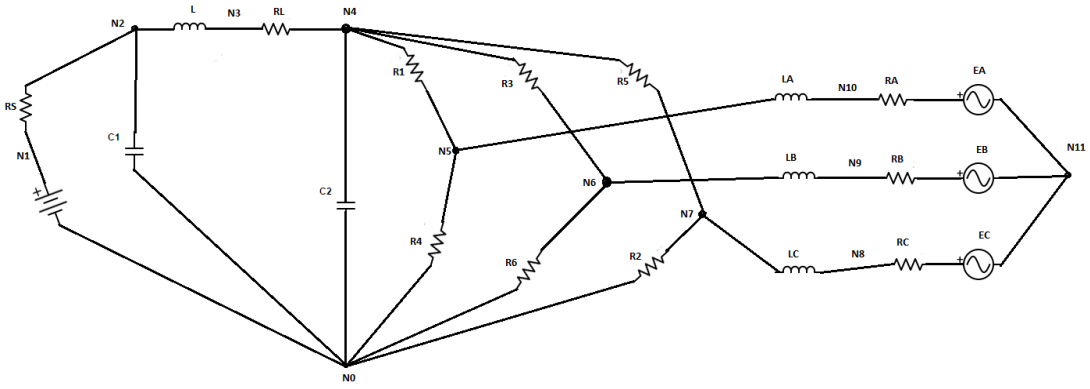

Figure 1.13: A lumped network, to evaluate the performance of the drive system of BLDC motor.

Where R_1, R_2, R_3, R_4, R_5 and R_6 are the internal resistances of the MOSFETs; R_A, R_B and R_C are the winding resistances; L_A, L_B and L_C are the winding inductances; E_A, E_B and E_C are the back EMFs.

$$\begin{bmatrix} U_{rn} \\ U_{gn} \\ U_{bn} \end{bmatrix} = \begin{bmatrix} R_r & 0 & 0 \\ 0 & R_g & 0 \\ 0 & 0 & R_b \end{bmatrix} \begin{bmatrix} i_r \\ i_g \\ i_b \end{bmatrix} + \frac{d}{dt} \begin{bmatrix} L_{rr} & L_{rg} & L_{rb} \\ L_{gr} & L_{gg} & L_{gb} \\ L_{br} & L_{bg} & L_{bb} \end{bmatrix} \begin{bmatrix} i_r \\ i_g \\ i_b \end{bmatrix} + \begin{bmatrix} \frac{d}{dt}\lambda_r \\ \frac{d}{dt}\lambda_g \\ \frac{d}{dt}\lambda_b \end{bmatrix} \quad (2.4)$$

Where U_{an}, U_{bn} and U_{cn} are the stator phase voltages; R_r , R_g and R_b are the stator resistances per phase; i_r, i_g and i_b are the stator phase currents; L_{rr}, L_{gg} and L_{bb} are the self-inductances of red, green and black phases respectively; L_{rg}, L_{gb} and L_{br} are the mutual inductances between red, green and black phases; $\frac{d}{dt}\lambda_r$,$\frac{d}{dt}\lambda_g$ and $\frac{d}{dt}\lambda_b$are the back electromotive forces for the respective phases.

$$\begin{bmatrix} U_{rn} \\ U_{gn} \\ U_{bn} \end{bmatrix} = \begin{bmatrix} R_r i_r \\ R_g i_g \\ R_b i_b \end{bmatrix} + \frac{d}{dt} \begin{bmatrix} L_{rr} i_r + L_{rg} i_g + L_{rb} i_b \\ L_{gr} i_r + L_{gg} i_g + L_{gb} i_b \\ L_{br} i_r + L_{bg} i_g + L_{bb} i_b \end{bmatrix} + \begin{bmatrix} \frac{d}{dt}\lambda_r \\ \frac{d}{dt}\lambda_g \\ \frac{d}{dt}\lambda_b \end{bmatrix} \quad (2.5)$$

When all the stator currents are balanced i.e.

$$i_r + i_g + i_b = 0 \quad (2.6)$$

During the fault on red phase $R_r \neq (R_g = R_b = R_{st})$ condition occurs. Rotor is in such a position that the current is going into red and out of green phase.

$$V_{rg} = v_{rn} - v_{gn} = i_r(R_r + R_g) + i_r\left(\frac{d}{dt}L_{rr} - 2\frac{d}{dt}i_{rg} + \frac{d}{dt}L_{gg}\right) + \frac{d}{dt}i_r\left(L_{rr} - 2L_{rg} + L_{gg}\right) + \frac{d}{dt}\lambda_r' - \frac{d}{dt}\lambda_g' \quad (2.7)$$

Where$\frac{d}{dt}\lambda_r$' and $\frac{d}{dt}\lambda_g'$ are the derivatives of the flux linkages (back electromotive forces) when phase imbalance occurs on the stator winding.

During the fault on black phase $R_b \neq (R_r = R_g = R_{st})$ condition occurs. Rotor is in such a position that the current is going into black and out of green phase.

$$V_{bg} = v_{bn} - v_{gn} = i_b(R_b + R_g) + i_b\left(\frac{d}{dt}L_{bb} - 2\frac{d}{dt}i_{bg} + \frac{d}{dt}L_{gg}\right) + \frac{d}{dt}i_b\left(L_{bb} - 2L_{bg} + L_{gg}\right) + \frac{d}{dt}\lambda_b' - \frac{d}{dt}\lambda_g' \quad (2.8)$$

Where$\frac{d}{dt}\lambda_r$' and $\frac{d}{dt}\lambda_g'$ are the derivatives of the flux linkages (back electromotive forces) when phase imbalance occurs on the stator winding.

Chapter - 3

Fault Detection using Electrical Signature Analysis

This section presents electrical signature analysis of stator currents of BLDC motor in order to assess and diagnose the health condition.

3.1 Stator current spectrum

Stator current spectrum can be used as an indication to the escalating fault condition in BLDC motor.

3.1.1 During healthy (unloaded) operating condition

Real time Fourier analysis has been performed on the digitalized signals obtained from the multi-function data acquisition board and saved in database for bench marking purpose. Electrical signature of the electrical motor has been obtained during healthy condition. Each harmonic has been processed and saved. Figure 3.1 shows the waveform of the stator current obtained through electrical signature analysis.

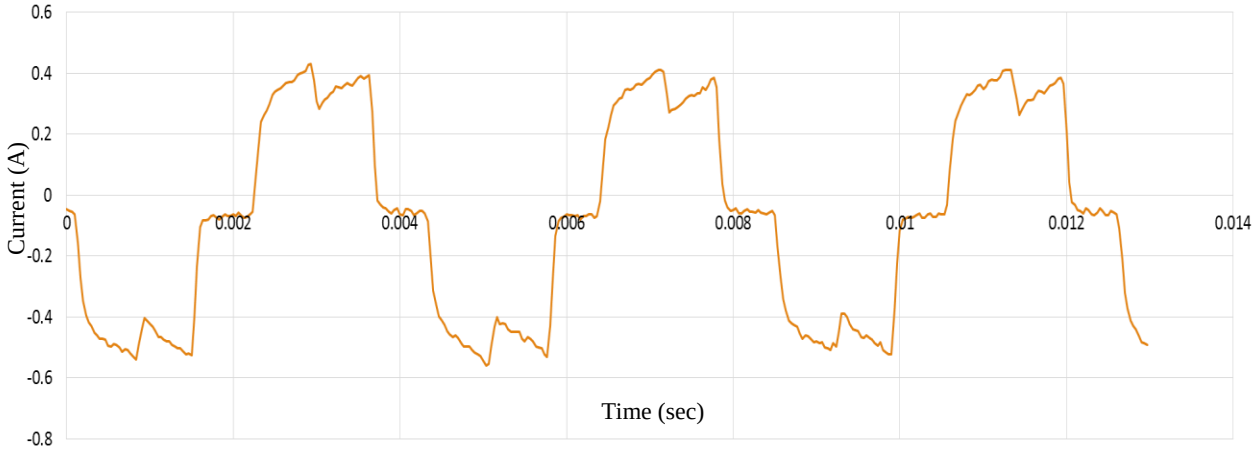

Figure 3.1: The stator current obtained through electrical signature analysis in healthy state.

Real time Fourier analysis has been performed using USB-6009 and LabVIEW system design software. Figure 3.1 shows the spectrum of the stator currents which confirms the absence of the all the triplen harmonics. The fundamental frequency of operation is 237 Hz. All the triplen harmonics i.e.711 Hz, 2133 Hz and so on are absent from the system.

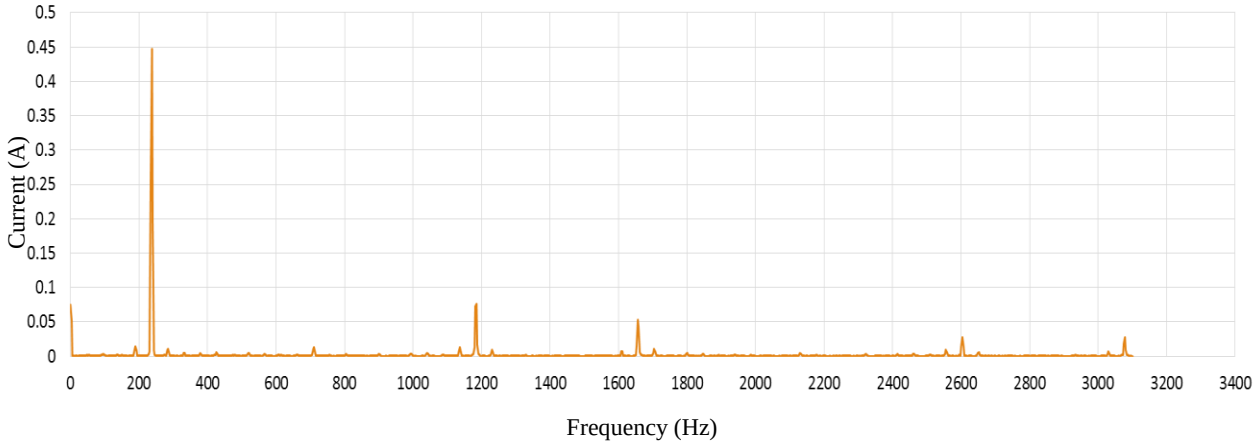

Figure 3.2: The spectrum of the stator currents in healthy condition.

Table 3.1 shows the normalized values of the harmonics obtained during the healthy condition of the BLDC motor. Normalized values of the triplen harmonics shows that their value is below 2 percent. This small value is due to the inherent mismatch present among the stator windings of the BLDC motor. Ideally there should not be any triplen harmonic under healthy test conditions.

Table 3.1: The normalized values of the harmonics obtained during the healthy condition.

Harmonic No.	**Harmonic normalized value**
Fundamental (237 Hz)	0.4470356
711 Hz 3rd Harmonic	0.0132058 (2%)
1185 Hz 5th Harmonic	0.0754786 (17%)
1659 Hz 7th Harmonic	0.0528861 (12%)
2133 Hz 9th Harmonic	0.0030561 (0.5%)
2607 Hz 11th Harmonic	0.0273015 (6.1%)

The total harmonic distortion of the BLDC motor obtained through the Table 3.1 is given by equation 3.1.

$$THD_i = \frac{\sqrt{\sum_{h=2}^{h_{max}} i_h^2}}{i_1} = 21.7\% \quad (3.1)$$

3.1.2 During healthy (loaded) operating condition

The Figure 3.3 shows the waveform of the stator currents during loaded condition. The loaded condition is produced by applying the electrical load on the DC series generator which in turn applies mechanical loading to BLDC motor. Hence varying dynamic mechanical stresses are applied to the motor.

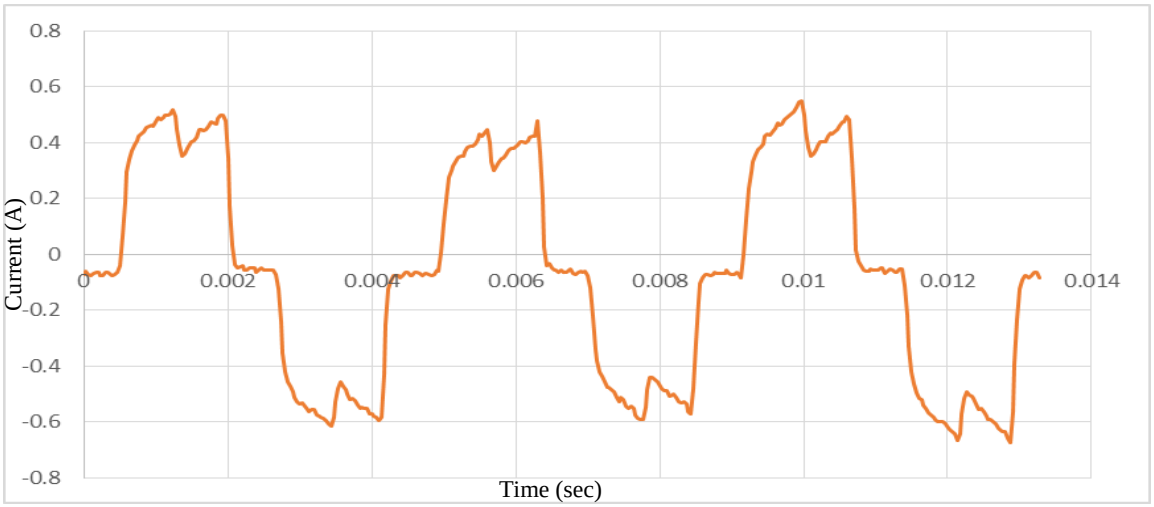

Figure 3.3: The waveform of the stator currents during loaded condition.

The spectrum of the stator currents of BLDC motor during healthy but loaded test condition is shown in Figure 3.4.

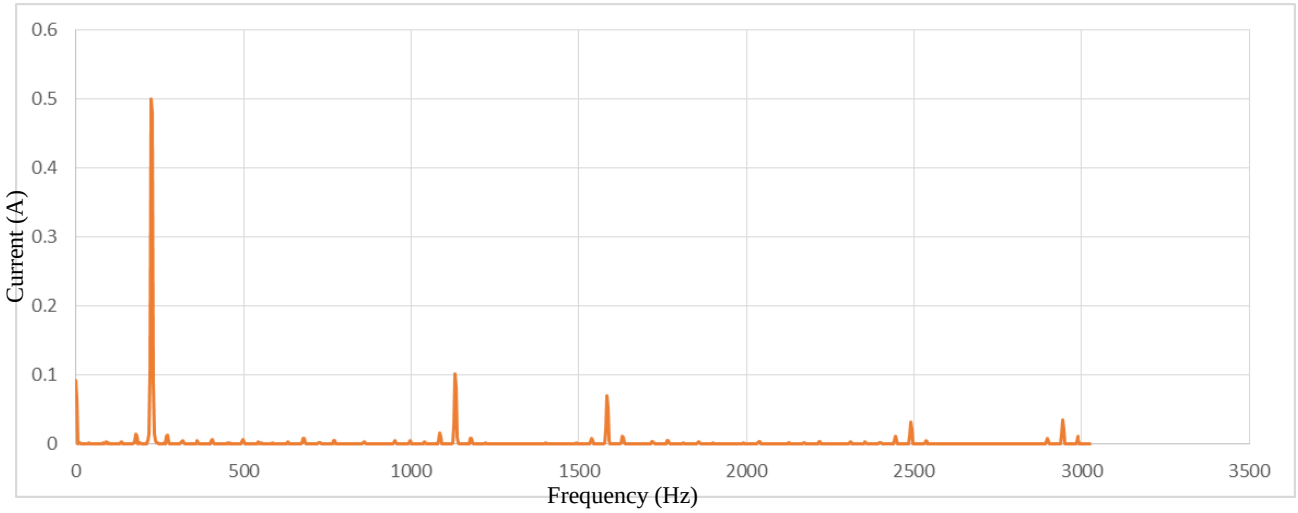

Figure 3.4: The spectrum of the stator currents of BLDC motor during healthy but loaded test condition.

The total harmonic distortion calculated is given by the equation 3.2. Total harmonic distortion gets increased to a value 25.6% from 21.7% when in loaded state.

$$THD_i = \frac{\sqrt{\sum_{h=2}^{h_{max}} i_h^2}}{i_1} = 25.6\% \quad (3.2)$$

3.1.3 During fault on black phase

We can see the overlapped waveforms in the Figure 3.5. The change in the frequency is due to the change in the resistance of the stator winding which in turn decreases the frequency of operation. The waveform with higher frequency of operation is the stator current waveform in the healthy condition. While the waveform with the less frequency of operation is, when the black phase is under fault condition.

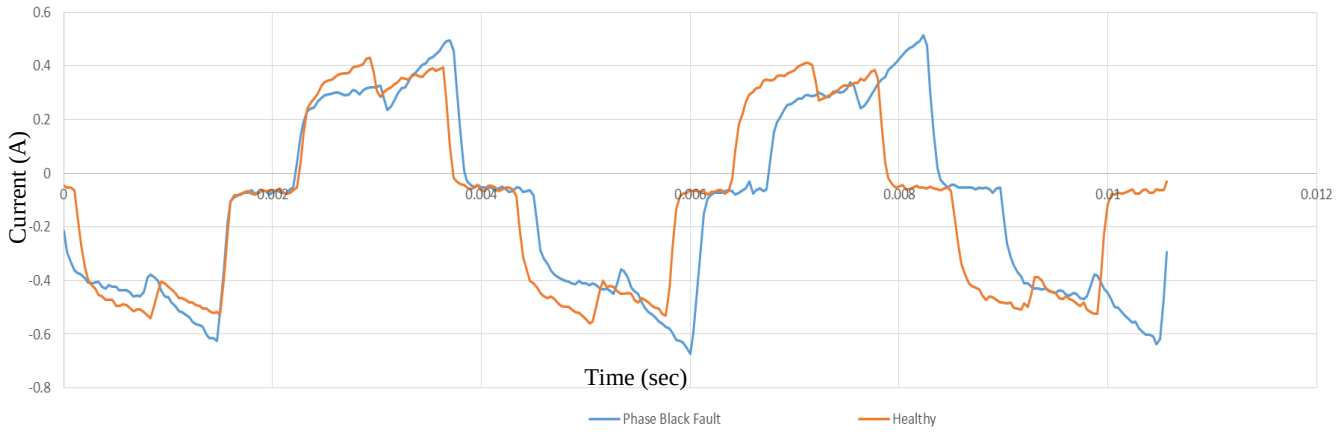

Figure 3.5: The over lapped waveforms under "healthy" and "phase black fault" conditions.

The spectrum of the stator currents during fault on the black phase as shown in Figure 3.6, indicates the presence of the triplen harmonics in the system. The 3rd harmonic during faulty condition on black phase escalates to 13% of normalized value. While the 9th harmonic has a value of 3%. Triplen harmonics grow into the system with the increase in the fault magnitude. As the phase imbalance raises, the value of these harmonics also get increased as given by equation 3.3. It is an

indication of the fault condition. The triplen harmonics are twice in value as compared to the healthy condition which is evident from the Table 3.2.

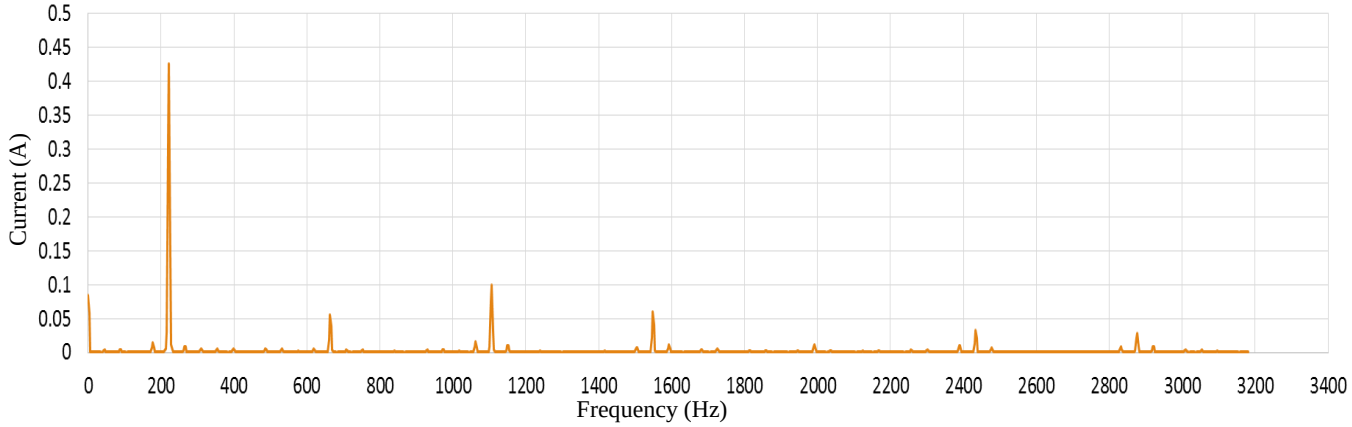

Figure 3.6: The spectrum of the stator currents during fault on the black phase.

The total harmonic distortion of the system during fault condition in now 31.3%. Which is higher than the total harmonic distortion as in the case of healthy condition.

$$THD_i = \frac{\sqrt{\sum_{h=2}^{h_{max}} i_h^2}}{i_1} = 31.3\% \qquad (3.3)$$

The Table 3.2 shows the normalized values of the harmonics under fault condition. If we compare this table with the Table 3.1, we can see the difference in the values.

Table 3.2: Shows the percentage of different harmonics present during fault on the black phase.

Harmonic No	**Harmonic value**
Fundamental (222 Hz)	0.4255067
666 Hz 3rd Harmonic	0.0551566 (13%)
1110 Hz 5th Harmonic	0.0998992 (23.47%)
1554 Hz 7th Harmonic	0.0593032 (14%)
1998 Hz 9th Harmonic	0.0114583 (3%)
2442 Hz 11th Harmonic	0.0327100 (8%)

3.1.4 During fault on red phase

When the red phase is subjected to fault it produces the same condition as in the case of the fault on the black phase. As this fault lies in the same category of single phase faults.

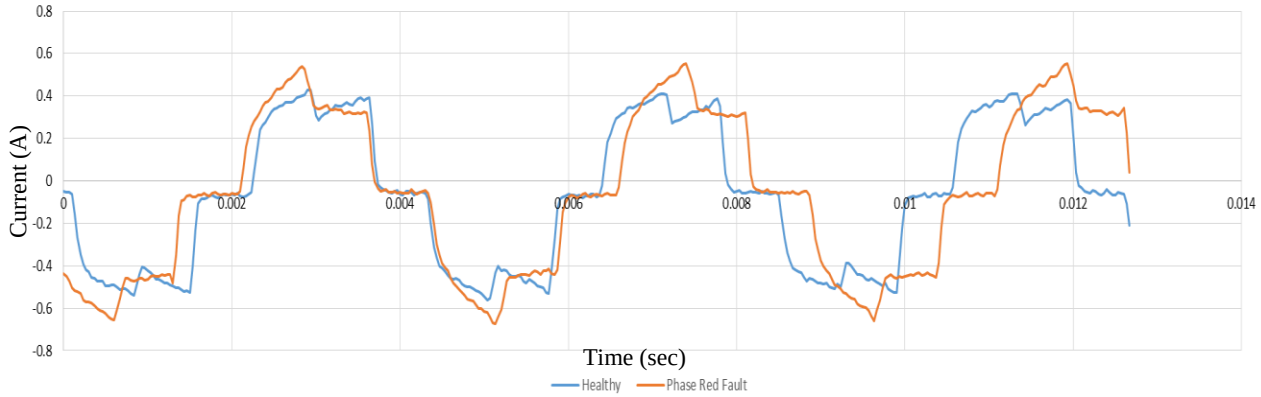

Figure 3.7: The harmonics of the single phase fault on the red phase.

The harmonics of the single phase fault on the red phase are shown in the Figure 3.7. Triplen harmonics are present in the stator currents of the BLDC motor. The 3rd harmonic has a contribution of 15% and 9th harmonic has a contribution of 3% which is quite higher in value as compared to healthy working condition of the BLDC motor as shown in Figure 3.8.

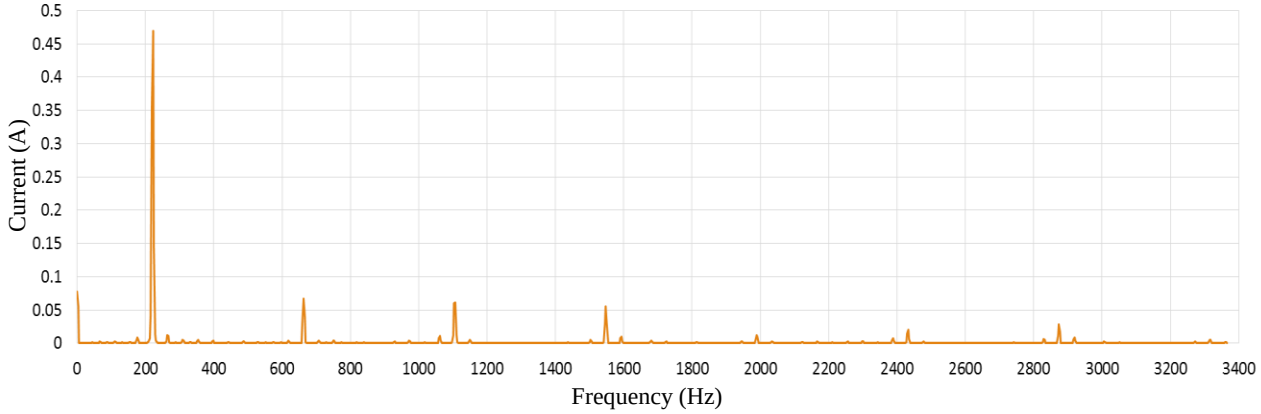

Figure 3.8: The spectrum of the stator current when red phase is subjected to fault.

The normalized values of the stator current harmonics are shown in Table 3.3. The 3rd harmonic has a contribution of 15% and 9th harmonic has a contribution of 3% in the spectrum of stator currents. It can be observed that as the fault occurs the harmonics escalates into the system.

Table 3.3: The normalized values of the stator current harmonics during fault on red phase.

Harmonic #	**Harmonic Value**
Fundamental (222 Hz)	0.469126598883732
666Hz 3rd	0.0666584850052231 (15%)
1110Hz 5th	0.061306395316485 (13%)
1554Hz 7th	0.055865704764107 (12%)
1998Hz 9th	0.0121083327851932 (3%)
2442Hz 11th	0.0200724009460748 (4.3%)

Total harmonic distortion is 25% as compared to 21.7% in the healthy condition as given by equation 3.4. It indicates that the THD increases as the fault condition escalates.

$$THD_i = \frac{\sqrt{\sum_{h=2}^{h_{max}} i_h^2}}{i_1} = 25\% \qquad (3.4)$$

3.1.5 During fault on white phase

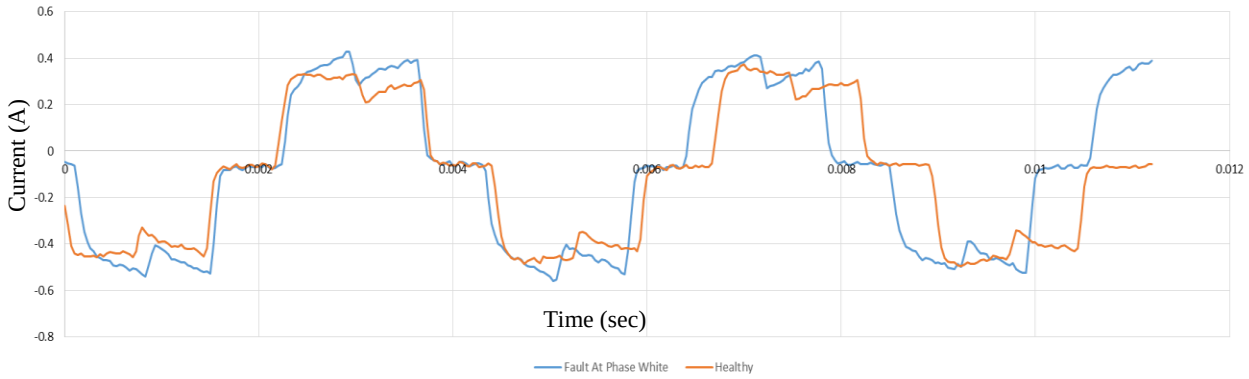

Figure 3.9: Harmonics obtained when a high impedance fault occurs on the white phase.

Figure 3.9 is obtained when a high impedance fault occurs on the white phase and we observe the harmonics at same phase. Table 3.4 shows that the 3rd harmonics has a contribution of 7.1% and 9th harmonic has a contribution of 2.5%. Other harmonics are also contributing toward total harmonic distortion as shown in Figure 3.10.

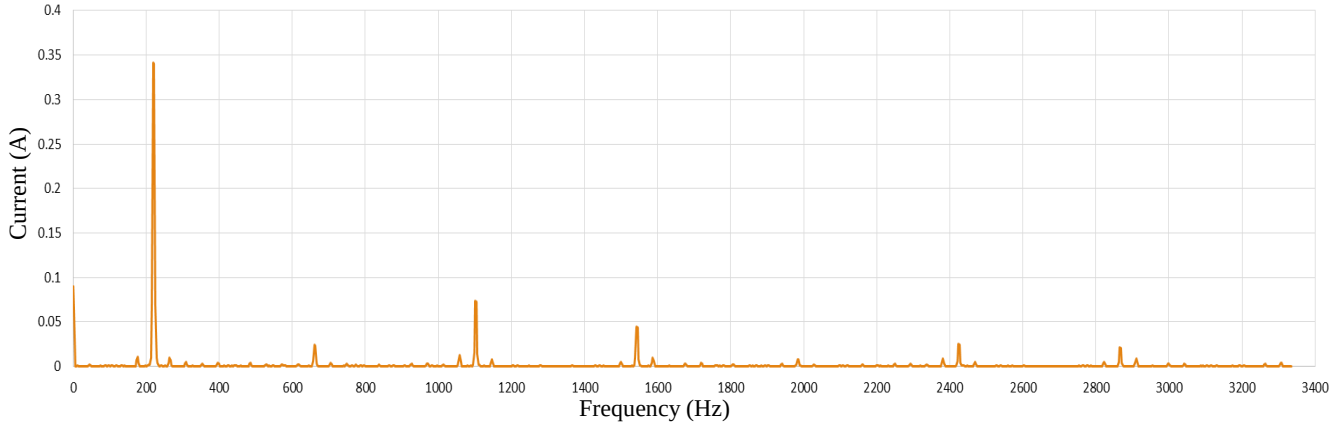

Figure 3.10: The spectrum of the stator current when white phase is subjected to fault.

Table 3.4: The normalized values of harmonics during fault on white phase.

Harmonic No.	**Harmonic value**
Fundamental (222 Hz)	0.340405213746
666 Hz 3rd Harmonic	0.024369632562 (7.1%)
1110 Hz 5th Harmonic	0.013451328248 (4%)
1554 Hz 7th Harmonic	0.044617049424 (13%)
1998 Hz 9th Harmonic	0.008133666550 (2.5%)
2442 Hz 11th Harmonic	0.025467455577 (7.5%)

3.1.6 During inter-turn fault

The other stator fault that can occur in the BLDC motor is the inter-turn fault. Figure 3.11 shows the waveform, when inter-turn fault occurs on a winding with 50 % of the winding is short circuited. Time domain signal during inter-turn fault do not show the visible difference from the waveform in healthy state but its spectrum clearly shows the difference. When dynamic

mechanical stresses are applied on the BLDC motor, Inter-turn short circuit could occur on the stator winding due to the continuous rubbing against the rotor.

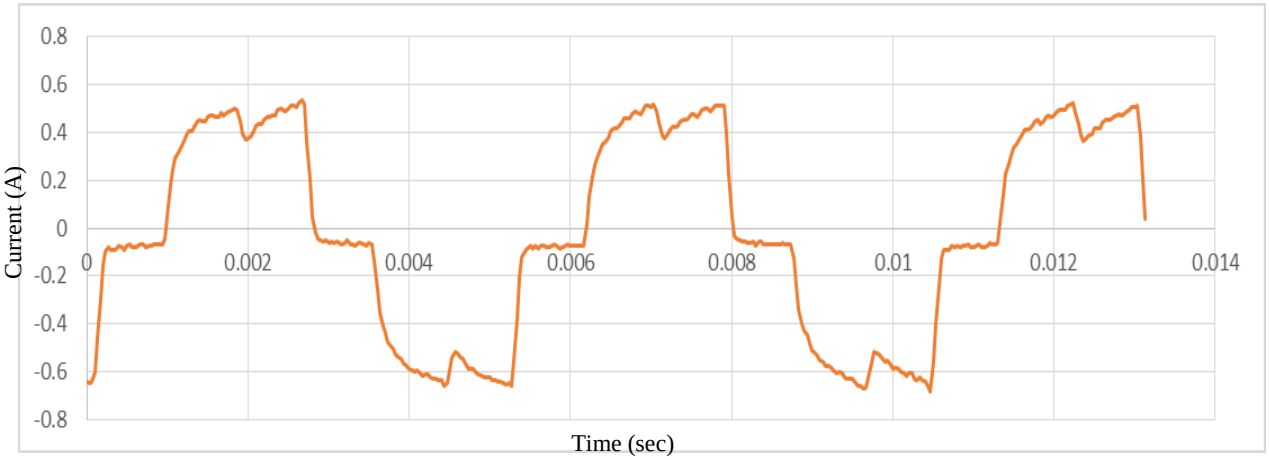

Figure 3.11: The waveform, when inter-turn fault occurs on a winding with 50% of the winding is short circuited.

The 3rd harmonic has a contribution of 13% and 9th harmonic has a contribution of 2.5% towards the total harmonic distortion.

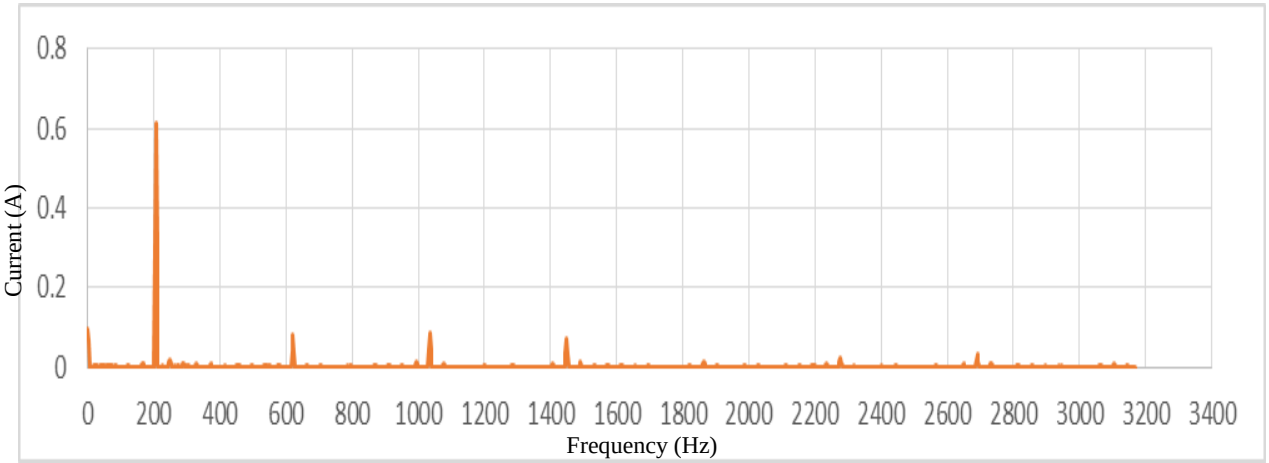

Figure 3.12: The spectrum, when inter-turn fault occurs on the BLDC motor stator winding.

Table 3.4 shows the normalized values of the stator current spectrum. All the harmonics are greater in magnitude in comparison with the healthy state harmonics. 3rd harmonic has contribution of 13% and 11th harmonic has a contribution of 2.3% towards total harmonic distortion.

Table 3.4: The normalized values of harmonics during inter-turn short circuit.

Harmonic No.	**Harmonic Value**
Fundamental (206 Hz)	0.612783272
618 Hz 3rd Harmonic	0.080240491 (13%)
1030 Hz 5th Harmonic	0.086766137 (14%)
1442 Hz 7th Harmonic	0.070826331 (12%)
1854 Hz 9th Harmonic	0.015120372 (2.5%)
2266 Hz 11th Harmonic	0.013574428 (2.3%)

3.1.7 During open circuit fault on black phase

Figure 3.13 shows when open circuit fault occurs on the BLDC motor system. Open circuit fault can occur either due to stator winding problem, lose connection problem or due to switch problem. It is clear from the diagram that when open circuit fault occurs all the harmonics escalates into the system. Even and odd bath harmonics are observed in this case.

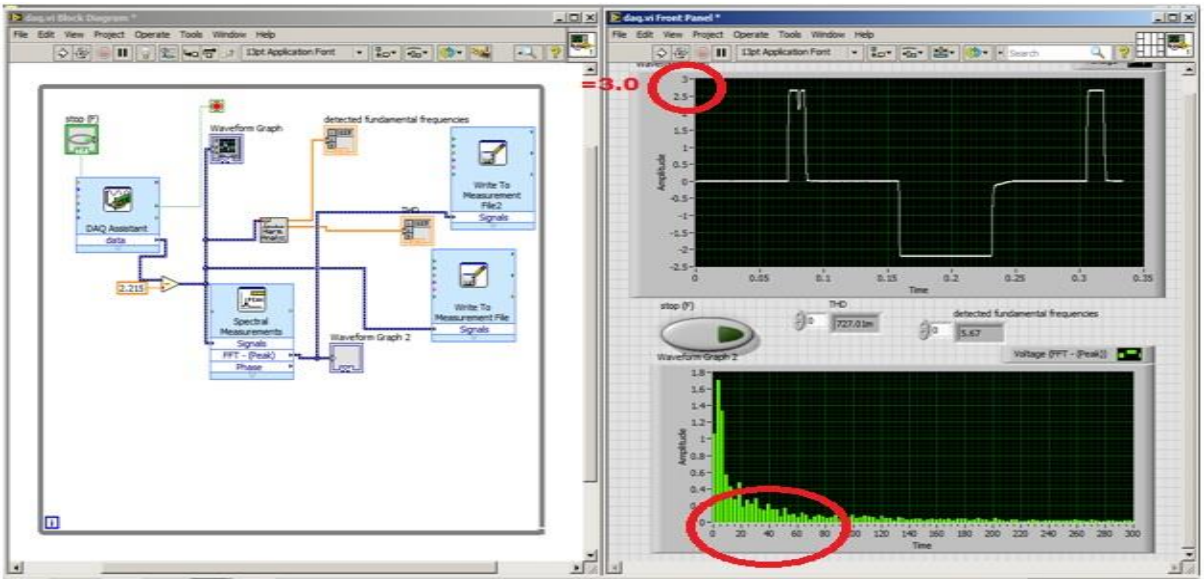

Fig. 3.13: The spectrum, when open circuit fault occurs on black phase of BLDC motor stator winding.

3.1.8 During open circuit fault on red phase

Figure 3.14 shows the spectrum and waveform of open circuit fault on the red phase of the BLDC motor. It has been observed that when open circuit fault occurs the frequency of operation reduced to a very small value in comparison with its normal frequency of operation. Peak value of the waveform approaches 3 to 4 times its healthy state. Both even and odd harmonics escalates into the spectrum of the stator currents. Which is a clear indication too the occurrence of the open circuit fault.

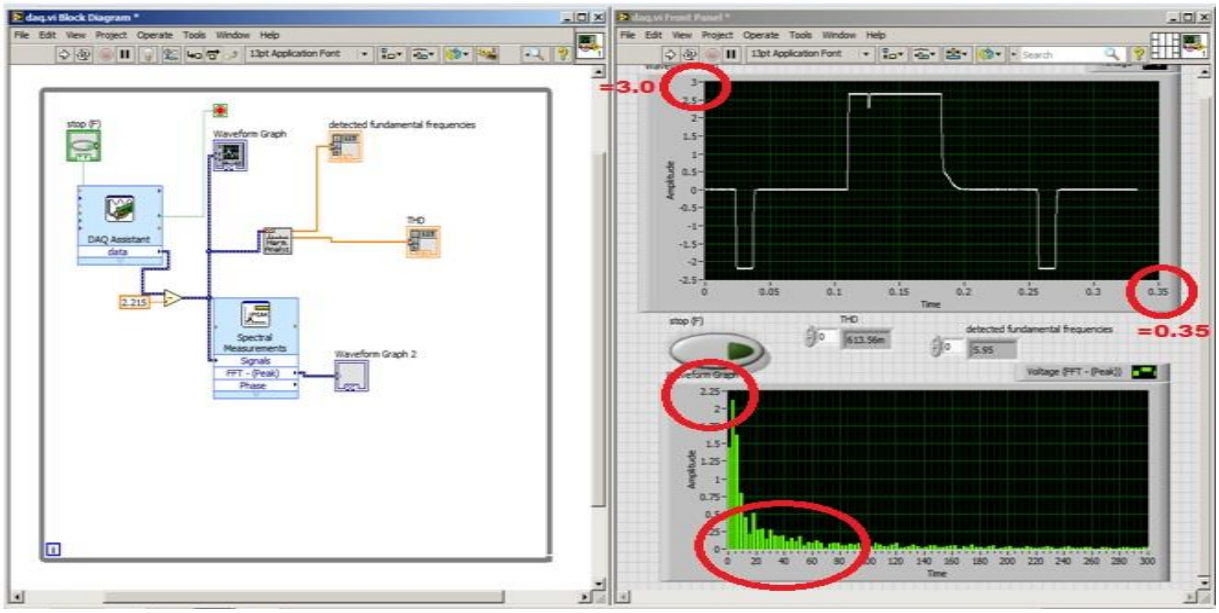

Fig. 3.14: The spectrum, when open circuit fault occurs on red phase of BLDC motor stator winding.

Chapter - 4

Implementation of Real Time Data Acquisition in LabVIEW and Comparison of Results

Comparative analysis of stator current of BLDC motor and their harmonics under different operating conditions are presented in the following chapter.

4.1 System design

LabVIEW system design software is used to implement real time data acquisition from the hardware. LabVIEW has an advantage of modular reconfigurable hardware in comparison to other software's that are used for data acquisition purposes.

4.1.1 Data acquisition and spectral measurements

Figure 4.1 shows the block diagram for the real time data acquisition and Fourier analysis. A time controlled loop is used for continuously acquiring the data from the USB-6009 hardware. The loop continuously scans the data available on its analogue input terminal and converts it into digital format. This data is available on the wired terminal of DAQ assistant. Then a spectral measurement unit is used to perform real time Fourier analysis on the signal obtained via DAQ assistant. To get the information about the fundamental frequency and total harmonic distortion the "harmonic analyzer module" is used. All these parameters are made available on the front view of LabVIEW.

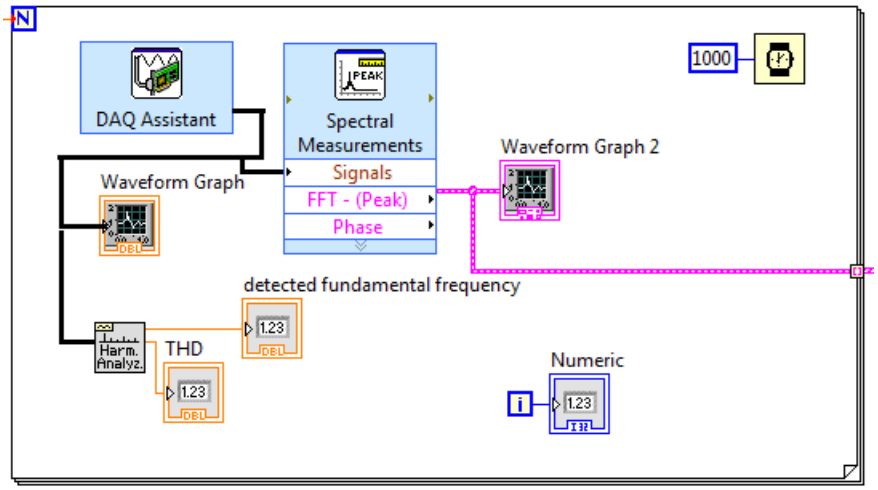

Figure 4.1: The block diagram for the real time data acquisition and Fourier analysis.

4.1.2 Serial interface

Serial port RS-232 interface is used for the communication of the data with the other modules of the software. The “Write buffer” writes the data on the VISA terminal of the serial interface and “Read buffer” reads the incoming data from the serial port and compares it with the already saved information in the code to perform a particular action. After comparison the decision is made and loop performs a particular task as shown in the Figure 4.2.

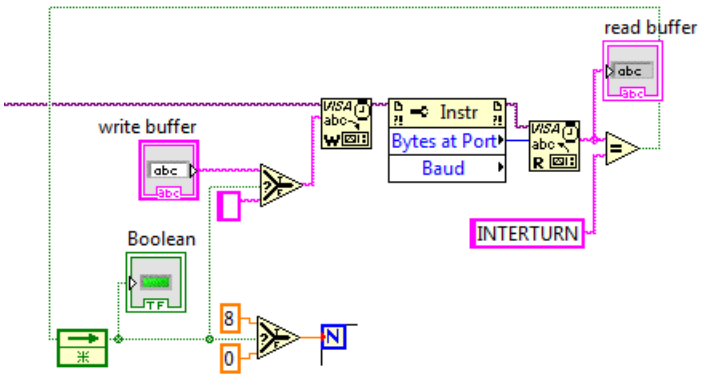

Figure 4.2: The block diagram of loop performing “Read” and “Write” operation.

4.1.3 Complete block diagram

Figure 4.3 shows the complete block diagram of the system to acquire data from the hardware and to perform real time Fourier analysis. The “Flat sequence structure” is used to initialize the serial port once. The “Write measurement file” is used for making real time database.

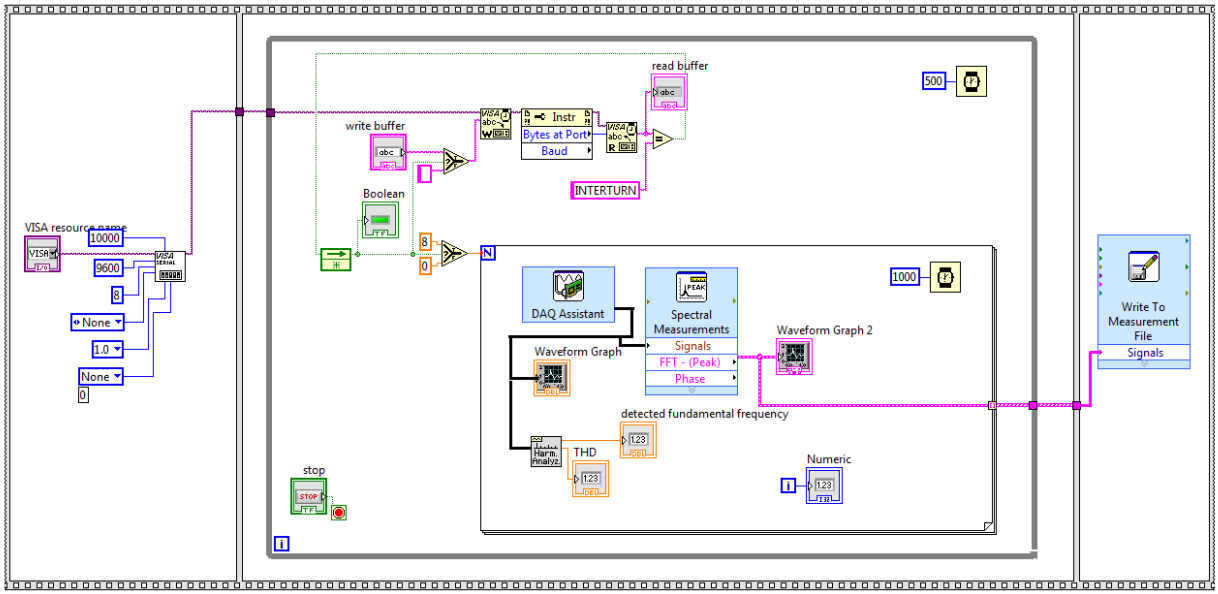

Figure 4.3: The complete block diagram of the system to acquire data from the hardware and to perform real time Fourier analysis.

4.2 Comparative analysis

The comparison of harmonic values of the faults under different conditions are presented in the following section.

4.2.1 Comparison during fault on red phase

Mechanical loading increases the total harmonic distortion in the spectrum of stator winding. It is observed that during healthy state the total harmonic distortion is 25.7% which is 4% more in value. Table 4.1 shows the comparative analysis of the harmonics in healthy state and when the stator winding is under high impedance fault. It is observed that there is a large difference between harmonics during healthy state and under fault condition. The 3rd harmonic has a contribution of

13% which is almost 7 times more than that in the healthy state. The 9th harmonic has a contribution of 3% which is 6 times more in value. Harmonics escalate into the system as the fault occurs.

Table 4.1: A comparative analysis of the harmonics in healthy state and when the stator winding is under high impedance fault.

Harmonic No.	**Harmonic value during fault**	**Healthy state harmonic**
Fundamental	0.4255067	0.4470356
3rd Harmonic	0.0551566 (13%)	0.0132058 (2%)
5th Harmonic	0.0998992 (23.47%)	0.0754786 (17%)
7th Harmonic	0.0593032 (14%)	0.0528861 (12%)
9th Harmonic	0.0114583 (3%)	0.0030561 (0.5%)
11th Harmonic	0.0327100 (8%)	0.0273015 (6.1%)

The total harmonic distortion obtained when the red phase of BLDC motor is under fault, has a contribution of 31.3% as confirmed by equation 4.1. Critical analysis of the Table 4.1 tells us about an increase in the total harmonic distortion. It is observed that there is a small amount of growth in the values of harmonics other than triplen harmonic. Such as 5th harmonic is 1.38 times more in value than in healthy state. Similarly, 7th harmonic is 1.16 times and 11th harmonic is 1.31 times more in value during faulty operating condition. So the major contribution towards the total harmonic distortion is due to the triplen harmonic. They get increased when the system is under imbalance condition. The 3rd harmonic is almost 7 times more in value than in healthy operating state of BLDC motor. Similarly, 9th harmonic is 6 times more in value.

$$THD_i = \frac{\sqrt{\sum_{h=2}^{h_{max}} i_h^2}}{i_1} = 31.3\% \quad (4.1)$$

Equation 4.2 calculates the value of total harmonic distortion in the stator currents of BLDC motor drive system.

$$THD_i = \frac{\sqrt{\sum_{h=2}^{h_{max}} i_h^2}}{i_1} = 21.7\% \quad (4.2)$$

4.2.2 Comparison during fault on black phase

BLDC motor has three-phases, so the fault could occur on any of it phase. Ideally speaking each phase should have same impedance i.e. phase to neutral and phase to phase resistance should be equal. Actually, it is not the case. As described in the chapter 2 article number 2.4, the resistance measured through precision micro-ohmmeter equipment of all three phases have different values. So every phase react differently to the fault. The Table 4.2 shows the scenario when the black phase of BLDC motor is under fault and the harmonics observed are on white phase. Indirectly, the effect of imbalance is observed on the white phase when the black phase is subjected to high impedance fault.

Fundamental harmonic is almost same is value. During healthy state of operation 5^{th} harmonic has maximum contribution towards the total harmonic distortion. After the fault occurs on the black phase, 3^{rd} harmonic has the maximum contribution towards the total harmonic distortion. There is not a much difference in the normalized values of harmonics other than triplen harmonic as shown in Table 4.2.

Table 4.2: The scenario when the black phase of BLDC motor is under fault and the harmonics are observed on the black phase.

Harmonic No.	**Harmonic value during fault**	**Healthy state harmonic**
Fundamental	0.469126598883732	0.4470356
3^{rd} Harmonic	0.0666584850052231 (15%)	0.0132058 (2%)
5^{th} Harmonic	0.061306395316485 (13%)	0.0754786 (17%)
7^{th} Harmonic	0.055865704764107 (12%)	0.0528861 (12%)
9^{th} Harmonic	0.0121083327851932 (3%)	0.0030561 (0.5%)
11^{th} Harmonic	0.0200724009460748 (4.3%)	0.0273015 (6.1%)

Total harmonic distortion has a contribution of 25.5% when the black phase is subjected to fault, as confirmed by the equation 4.3. Critical analysis of the Table 4.2 tells us about the cause of the increase in the total harmonic distortion. Fundamental harmonic has almost same value. The 3^{rd}

harmonic is more than 7 times in value than during at healthy state. Similarly, 9th harmonic is 6 times more in value during the faulty operating condition.

$$THD_i = \frac{\sqrt{\sum_{h=2}^{h_{max}} i_h^2}}{i_1} = 25\% \quad (4.3)$$

Equation 4.4 tells us the value of total harmonic distortion in the stator currents of BLDC motor when the black phase is subjected to fault.

$$THD_i = \frac{\sqrt{\sum_{h=2}^{h_{max}} i_h^2}}{i_1} = 21.7\% \quad (4.4)$$

4.2.3 Comparison during fault on white phase

Table 4.3 shows the scenario when the fault is subjected to white phase of the BLDC motor and harmonics are observed on the same phase. Same results are obtained in this case. Triplen harmonic have a major contribution towards the total harmonic distortion. All other harmonics do not escalate into the spectrum of the stator currents at the same rate like triplen harmonic. 3rd harmonic is more than 6 times in value than at healthy state of operation. Similarly, 9th harmonic is almost 5 times in value.

Table 4.3: The scenario when the fault is subjected to white phase of the BLDC motor and harmonic are observed on the same phase.

Harmonic No.	**Harmonic value during fault**	**Healthy state harmonic**
Fundamental	0.6127832729	0.4470356
3rd Harmonic	0.0802404914 (13%)	0.0132058 (2%)
5th Harmonic	0.0867661376 (14%)	0.0754786 (17%)
7th Harmonic	0.0708263313 (12%)	0.0528861 (12%)
9th Harmonic	0.0151203722 (2.5%)	0.0030561 (0.5%)
11th Harmonic	0.0135744280 (2.3%)	0.0273015 (6.1%)

Total harmonic distortion has a contribution of 23% when the white phase is subjected to fault, and harmonics are observed on the same phase, as confirmed by the equation 4.5. Critical analysis of the Table 4.3 shows the cause of the increase in the total harmonic distortion.

$$THD_i = \frac{\sqrt{\sum_{h=2}^{h_{max}} i_h^2}}{i_1} = 23\% \quad (4.5)$$

Equation 4.6 shows the contribution of harmonics when the BLDC motor is working in healthy state.

$$THD_i = \frac{\sqrt{\sum_{h=2}^{h_{max}} i_h^2}}{i_1} = 21.7\% \quad (4.6)$$

Total harmonic distortion is used in conjunction with Fourier spectrum to assess the severity of fault. Total harmonic distortion escalates into the system as the fault occurs.

Conclusion

It has been theoretically verified and experimentally confirmed that brushless DC (BLDC) motor faults can be identified at initial stages by spectrum of the stator currents. Electrical signature analysis (ESA) technique is invisible to monitored device in comparison to vibration analysis based technique that needs accelerometers and other associated equipment.

It has been empirically verified that all BLDC stator faults produces an imbalance scenario which results in an increase in total harmonic distortion on the spectrum of stator currents.

Electrical signature analysis of healthy BLDC motor confirms the absence of 3^{rd} and 9^{th} harmonic from the spectrum of the stator current. When stator winding is subjected to fault, triplen harmonics escalates into the signatures of stator current, which could be used as a warning to incipient fault condition.

Moreover, an increase in total harmonic distortion is observed during varying mechanical stresses on the BLDC motor. While, vibration analysis based monitoring technique is considered to be more reliable, but it does not give any information on electrical characteristics of BLDC motor.

Appendices

Supply Voltages

$$U_a = 240\ volts \quad (1)$$

$$U_{L-L} = \sqrt{3} \times U_a = 415\ volts \quad (2)$$

DC link voltage

$$V_{dc} = \sqrt{2} \times U_{L-L} = \sqrt{2} \times (415) = 586.89 \quad (3)$$

$$V_{dc} = 600\ Volts \quad (4)$$

$$E = P \times T \quad (5)$$

References

[1]. P. Yedamale, "Brushless DC (BLDC) Motor Fundamentals", Microchip Technology, 2007 [Online], available: http://ww1.microchip.com /downloads /en/ppNotes/00885a.pdf

[2]. Y. S. Jeon, H. S. Mok, G. H. Choe and D. K. Kim, "A new simulation model of BLDC motor with real back EMF waveform", Proceedings of Computers in Power Electronics, Blacksburg (USA), pp. 217-220, Jul. 2000

[3]. C. Kral, T. G. Habetler, and R. G. Harley, "Detection of mechanical imbalances of induction machines without spectral analysis of time-domain signals", Proceedings of IEEE Transaction on Industry Applications, Vol. 40, pp. 1101-1106, July-Aug. 2004.

[4]. S. Rajagopalan, T. G. Habetler, R. G. Harley, T. Sebastian, B. Lequesne, "Current/Voltage based detection of faults in gear coupled to electric motors", Proceedings of IEEE transaction on industry applications, Vol. 42, pp. 1780-1787, July. 2006

[5]. G. H. Jang, J. H. Park and J. H. Chang, "Position detection and start-up algorithm of a rotor in a sensorless BLDC motor utilising inductance variation", Proceedings of IEEE transaction On Electric Power Applications, Vol. 149, pp. 137-142, Mar. 2002.

[6]. S. Rajagopalan, J. M. Aller, J. A. Restrepo, T. G. Habetler and R. G. Harley, "Detection of Rotor Faults in Brushless DC Motors Operating Under Non-stationary Conditions", Proceedings of IEEE Transaction on Industry Applications, Vol. 42, pp. 1464 – 1477, Nov.-Dec. 2006

[7]. Yoon Taeyong, "Magnetically induced vibration in a permanent-magnet brushless DC motor with symmetric pole-slot configuration", Proceedings of IEEE Transaction on Magnetics, Vol. 41, pp. 2173 – 2179, June 2005

[8]. Li Jianjun, Xu Yongxiang and Zou Jibin, “A study on the reduction of vibration and acoustic noise for brushless DC motor”, Proceedings of International Conference on Electrical Machines and Systems ,Wuhan (China), pp. 561 – 563, Oct. 2008

[9]. S. Rajagopalan, T. G. Habetler, R. G. Harley, T. Sebastian and B. Lequesne, “Current/Voltage Based Detection of Faults in Gears Coupled to Electric Motors”, Proceedings of IEEE Transaction on Industry Applications, Vol. 42, pp. 1412 – 1420, Nov.-Dec. 2006

[10]. Satish Rajagopalan, Wiehan le Roux, Thomas G. Habetler, and Ronald G. Harley, “Dynamic eccentricity and demagnetized rotor magnet detection in trapezoidal flux (brushless dc) motors operating under different load conditions,” Proceedings of IEEE Transaction On Power Electronics, Vol. 22, pp. 2061 – 2069, Sept. 2007

[11]. Jongman Hong, Sanguk Park, Doosoo Hyun, Tae-june Kang, Sang Bin Lee, Kral C and Haumer A, "Detection and Classification of Rotor Demagnetization and Eccentricity Faults for PM Synchronous Motors", Proceedings of IEEE Transactions on Industry Applications, Vol. 48, pp. 923 – 932, May-June 2012

[12]. J. F. Zubizarreta, J. F. Rodriguez, S. Vasudevan, "Condition monitoring of brushless DC motors with non-stationary dynamic conditions", Proceedings of International Conerence on Instrumentation and Measurement Technology (I2MTC), Montevideo (Uruguay), pp.: 62 – 67

[13]. S. Rajagopalan, J. M. Aller, J. A. Restrepo , T. G. Habetler and R. G. Harley, “Detection of Rotor Faults in Brushless DC Motors Operating Under Nonstationary Conditions,” Proceedings of IEEE Transaction on Industry Applications, Vol. 42, pp. 1464 – 1477, Nov.-Dec. 2006

[14]. A. Mohamed, M. Awadallah, Morcos, Suresh Gopalakrishnan, and W. Nehl Thomas "Detection of Stator Short Circuits in VSI-Fed Brushless DC Motors Using Wavelet Transform", Proceedings of IEEE Transaction On ENERGY CONVERSION, Vol. 21, pp. 1 – 8, March 2006

[15]. R. M. Tallam, T. G. Habetler, and R. G. Harley, "Stator winding turn fault detection for closed-loop induction motor drives", Proceedings of IEEE Transaction on Industrial Applications, Vol. 39, pp. 720–724, May-Jun. 2003.